10.1515/astro-2017-0138

Baltic Astronomy, vol. 25, 324–330, 2016

MOLECULAR CLOUDS AND STAR FORMATION RATE IN DISK GALAXIES

E. O. Vasiliev[1,2], S. A. Khoperskov[3,4] and A. V. Khoperskov[5]

[1] *Southern Federal University, Sorge 5, Rostov on Don, 344090 Russia*

[2] *Special Astrophysical Observatory, Russian Academy of Sciences, Nizhnii Arkhyz, Karachaevo-Cherkesskaya Republic, 369167 Russia*

[3] *GEPI, Observatoire de Paris, CNRS, Université Paris Diderot, 5 place Jules Janssen, 92190 Meudon, France*

[4] *Institute of Astronomy, Russian Academy of Sciences, Pyatnitskaya st., 48, Moscow, 119017 Russia*

[5] *Volgograd State University, Universitetsky pr. 100, Volgograd, 400062 Russia*

Received: 2016 September 27; accepted: 2016 October 17

Abstract. We use N-body/hydrodynamic simulations of a Milky Way-like galaxy to study the physical properties of giant molecular clouds and star formation rate on different spatial scales. We confirm the previous estimates that the dark gas fraction in molecular clouds reaches about 30% by mass. We find that conversion factors for individual molecular clouds deviated by a factor of several times from the mean value for the Milky Way clouds, $X_{\rm CO} = 2 \times 10^{20}$ cm^{-2} (K km s^{-1})$^{-1}$, and hence a constant $X_{\rm CO}$ conversion factor cannot represent the physical properties of an individual molecular cloud or a small sample of clouds sufficiently well, but the conversion factor averaged over the whole ensemble of clouds is believed to be close to the Milky Way value. The $\Sigma_{\rm SFR}^{\rm UV} - \Sigma_{\rm gas}$ relation can be reproduced using UV calibration for smoothing scale compared to the size of individual star-forming complexes, $\sim 0.3 - 1$ kpc.

Key words: ISM: clouds – ISM: molecules – ISM: structure – stars: formation – galaxies: spiral – galaxies: structure

1. INTRODUCTION

Molecular clouds are believed to be regions of intense star formation (see the review by Kennicutt & Evans 2012). Because of high temperature required for excitation of molecular hydrogen rotational transitions the major part of H_2 gas in galaxies remains invisible and one should use CO lines as a tracer of molecular gas. The standard methodology uses a simple relationship between the observed CO intensity and the column density of molecular gas: $N_{\rm H_2} = X_{\rm CO} W_{\rm CO}$. The conversion factor $X_{\rm CO}$ is usually assumed to be constant, but recent studies argue that it depends on physical parameters inside the clouds and environmental effects (see, e.g., Bolatto et al. 2013). This may lead to incorrect estimates of molecular gas mass in a galaxy. However, more significant uncertainty comes from the fragility of CO molecule and the difference in formation time scales of H_2 and CO

molecules (Shchekinov 2004; Wolfire et al. 2010). Furthermore, a part of molecular gas remains unaccounted for in the standard methodology for determining the mass of H_2 gas in galaxies. Such gas is called dark gas, its fraction can be as high as $\sim 30\%$ of the total molecular gas in a galaxy (Shchekinov 2004; Wolfire et al. 2010). This factor inevitably affects estimates of star formation, given the well-established Kennicutt-Schmidt relation between the surface star formation rate (SFR) and gas surface density (Schmidt 1959; Kennicutt 1998). SFR can be estimated using several calibrations based on available data sets (optical/UV, mid-far IR, H I, CO). This relation is usually presented in a global form, i.e., in terms of disk-averaged surface SFR and gas surface density in galaxies (Kennicutt 1998), whereas star formation is associated with molecular clouds whose physical parameters depend on their location in a galaxy (Colombo et al. 2014; Khoperskov et al. 2016) and which have sizes smaller than 1 kpc.

Here we study how the conversion factor varies in molecular clouds and then calculate the dark gas fraction in clouds, study star formation rate on small spatial scales and investigate how local effects change the Kennicutt-Schmidt relation. The paper is organized as follows. In Section 2 we describe our numerical models in brief. Section 3 presents our calculations of dark molecular fraction in clouds. Section 4 describes the "surface SFR density – gas surface density" relation on sub-kpc scales. Section 5 summarizes our results.

2. MODEL AND CLOUD PARAMETERS

To simulate the galaxy evolution we use our code based on the unsplit TVD MUSCL (Total Variation Diminishing Multi Upstream Scheme for Conservation Laws) scheme for gas dynamics and the N-body method for stellar component dynamics. Stellar dynamics is calculated using the second order flip-flop integrator. For the total stellar-gaseous gravitational field calculation we use the TreeCode approach. For a detailed description of these numerical methods, see Khoperskov et al. (2014, 2016). We implemented the self-consistent cooling/heating processes (Khoperskov et al. 2013) coupled with the chemical evolution of 20 species including CO and H_2 molecules, using a simplified chemical network described by Nelson & Langer (1999). In the star formation recipe adopted in our model, the mass, energy and momentum from the gaseous cells where star formation criterion is satisfied are transferred directly to newborn stellar particles. To compute UV emission radiated by stellar population we use the stellar evolution code STARBURST99 (Leitherer et al. 1999), assuming solar metallicity of stellar population. We transfer the UV radiation from young stars using a simple ray-tracing method. Further details of our numerical model can be found in Khoperskov et al. (2016).

We start our simulations from the self-consistent radial and vertical equilibrium state of stellar-gaseous disks in a fixed gravitational potential of dark matter halo. A variation of initial parameters (e.g., halo scale length, gas velocity dispersion, etc.) allows us to follow galaxies with different morphology. In the previous paper (Khoperskov et al. 2016) we studied molecular cloud properties in galaxies with a gravitationally stable disk (Model F, without prominent structure), highly unstable disk (Model H, flocculent spiral morphology) and intermediate-state disk (Model B, MW-like morphology). Here we consider a disk galaxy with a bar and four spiral arms – Model B. Fig. 1 presents gas surface density $\Sigma_{\rm gas}$, stellar surface density $\Sigma_{\rm stars}$, and integrated CO intensity $W_{\rm CO}$ for a galaxy in Model B.

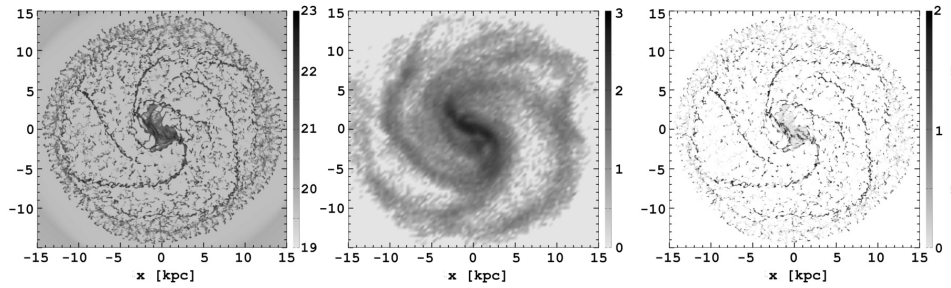

Fig. 1. Gas surface density $\Sigma_{\rm gas}$ (*left-hand panel*), stellar surface density $\Sigma_{\rm stars}$ (*middle panel*), and integrated CO intensity $W_{\rm CO}$ (*right-hand panel*) for a galaxy in Model B.

3. DARK MOLECULAR GAS

On physical grounds, the border of a molecular cloud should be found by using some relation between the gas volume density and molecular fraction, however, because most observations can measure only surface densities and velocity structure along the line of sight we apply a similar technique here. In general, a cloud can be defined in several ways. A comparison of physical properties of molecular clouds extracted by different methods can be found in Khoperskov et al. (2016), Duarte-Cabral & Dobbs (2016), and Pan et al. (2016). We use the CLUMPFIND package (Williams et al. 1994) to identify an ensemble of molecular clouds for a given CO brightness temperature level, here we assume it to be equal to $T_{\rm th}^{\rm b} = 3$ K. Fig. 1 (the right-hand panel) presents the distribution of integrated CO intensity, $W_{\rm CO}$, over the galactic disk. We thus have for each cloud the distributions of surface density, CO luminosity, and other parameters, and this allows us to calculate the virial mass. First of all, we look on how the conversion factor varies for clouds in the ensemble. Fig. 2 (the left-hand panel) shows the dependence of the mean conversion factors $X_{\rm CO}$ on the column density values $N_{\rm H2}$ for each cloud in the ensemble. One can note a remarkable scatter of conversion factor not only about the mean value for the MW clouds, $X_{\rm CO} \sim 2 \times 10^{20}$ cm^{-2} (K km s^{-1})$^{-1}$ (Bolatto et al. 2013), but also about the theoretical value predicted by Feldmann et al. (2012). The mean factor for most of the clouds deviates by about $\pm 30\%$ from that for the MW clouds, but the difference is as large as a factor of several times for a significant number of clouds. Certainly, such deviations should show up in the mass of a cloud calculated from CO luminosity: $M_{\rm cl}^{*} \sim X_{\rm CO} L_{\rm CO}$ (see, e.g., Eq. 7 in Colombo et al. 2014). Because the scatter of the conversion factor about the MW value is non-symmetric, but tends to be close to it, a conversion factor averaged over the whole ensemble of clouds is expected to be close to the MW value (the difference between the total mass estimated using individual conversion factors for each cloud and the estimate computed for the MW value will be studied elsewhere). Therefore, we take the MW value for the conversion factor in our further calculations.

Molecular clouds are usually assumed to be virilized objects. The virial mass of a cloud, $M_{\rm cl}$, depends on its density profile, and if we adopt $\rho \sim r^{-1}$ then the virial mass becomes $M_{\rm cl} \sim \sigma^2 R$, where R is the cloud radius, and σ is the velocity dispersion (e.g., Colombo et al. 2014). We can then compare these mass values for each cloud and find the difference, which reflects the amount of dark gas in CO

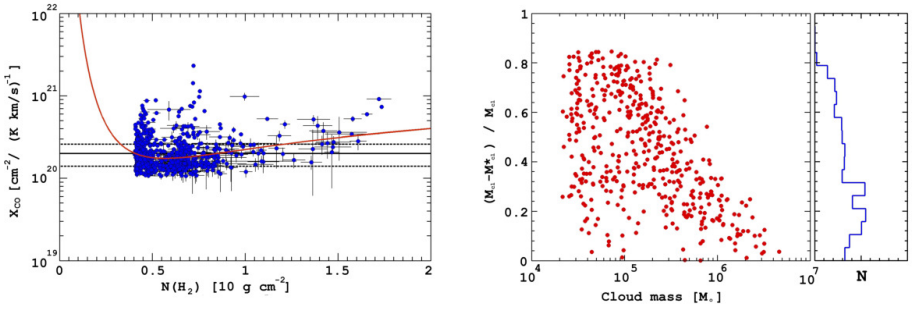

Fig. 2. *Left-hand panel.* Mean conversion factor $X_{\rm CO}$ versus mean column density. Each point corresponds to an isolated molecular cloud. The error bars show the ranges of $X_{\rm CO}$ and $\Sigma_{\rm cl}$ values within a cloud. The horizontal lines indicate the mean Milky Way $X_{\rm CO}$ value (solid line) and $\pm 30\%$ deviation from the mean value (dashed lines). The solid curve shows the theoretical dependence predicted by Feldmann et al. (2012). *Right-hand panel.* The dependence of the fraction of dark component in a molecular cloud on the virial mass of the cloud, $M_{\rm cl}$. The histogram of the distribution of clouds by the dark-component fraction is shown in a separate frame on the right.

lines if molecular clouds are assumed to be virialized. This difference represents the uncertainty in calculating the mass of a cloud. Fig. 2 presents the fraction of dark gas for each molecular cloud: $(M_{\rm cl} - M^*_{\rm cl})/M_{\rm cl}$. One can note the large scatter (from almost zero to ~ 0.8) of this fraction and the lack of dependence on the mass of a cloud for $M_{\rm cl} < 3 \times 10^5\ M_\odot$. For more massive clouds the fraction becomes smaller and for $M_{\rm cl} \sim 3 \times 10^5\ M_\odot$ it drops down to less than 0.1. However, clouds with the dark-gas fraction less than 0.4 dominate by number (see the histogram in the right-hand panel of Fig. 2). Therefore, the dark-gas fraction averaged by the number of clouds is about 30%, and hence agrees with both semi-analytic (Shchekinov 2004; Wolfire et al. 2010) and numerical (Smith et al. 2014) studies. One should mention that a major part of the clouds, up to 70%, is expected to be unvirialized (Shchekinov 2004), implying that the dark-gas fraction should be significantly underestimated due to both the low surface density and the low CO fraction in such gas.

4. SFR ON DISK- AND SUB-KPC SCALES

A power-law relation between the surface SFR and gas surface density – the Schmidt law (Schmidt 1959) – was originally stated in global form by Kennicutt (1998). This form means that the related values are averaged over the whole galactic disk. However, star formation takes place on much smaller scales. On the other hand, a study of star formation on very small scales leads to inappropriate picture because the molecular clouds and OB clusters are several dozens of parsecs in size. We may them consider as a region populated by either molecular gas or stellar cluster, or pick up too small OB cluster, resulting in underestimated UV or Hα emission from this region. A study of star formation on small scales becomes possible due to the increase of spatial resolution, and is of great interest because individual star-forming complexes are taken into account, whose sizes are $\sim 0.3 - 1$ kpc (Efremov 1995).

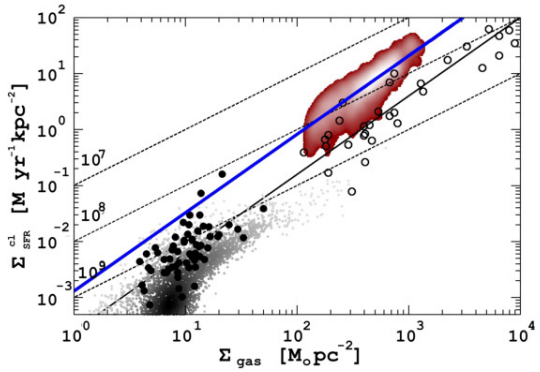

Fig. 3. Relation between SFR surface density, $\Sigma^{\rm cl}_{\rm SFR}$, and total (atomic and molecular) gas surface density, $\Sigma_{\rm gas}$. The SFR is calculated by Eq. 1. The grayscale points correspond to the extragalactic observations by Bigiel et al. (2010). The big circles represent the data adopted from Kennicutt (1998): each point represents an individual galaxy, the filled and open symbols correspond to normal-disk and starburst galaxies, respectively. The thin solid line shows a fit to the data (Kennicutt 1998). The thick solid line represents the fit with a slope $N = 1.4$ for the simulated set of molecular clouds. The thin dotted lines correspond to gas consumption timescales (see labels, time in yrs) for a constant global star formation efficiency of 10%.

Basically, star formation rate in a collapsing cloud can be found as

$$\Sigma^{\rm cl}_{\rm SFR} \propto M_{\rm cl} t_{\rm ff}^{-1}\,, \tag{1}$$

where $t_{\rm ff}$ is free fall time. Fig. 3 shows a remarkable agreement of our data (red/grey region) and the loci of points for starburst galaxies (Kennicutt 1998).

On the other hand, SFR can be estimated using several calibrations in different wavelengths, from radio to X-ray (e.g., Kennicutt & Evans 2012). Young stars emit enormous number of UV photons, and hence high UV flux is inherent to regions with ongoing star formation, and then UV flux is expected to be used for SFR calibration (Kennicutt 1998):

$$\Sigma^{\rm UV}_{\rm SFR} \propto L_{\rm UV}\,. \tag{2}$$

Given our discussions about the size of star formation regions, it is interesting to compare the $\Sigma^{\rm cl}_{\rm SFR} - \Sigma_{\rm gas}$ relation obtained from (1) with the $\Sigma^{\rm UV}_{\rm SFR} - \Sigma_{\rm gas}$ relation calculated using UV flux as calibration (2). For this purpose, we convolve the simulated gas density and UV flux maps with a Gaussian filter with a beam size ranging from 100 to 800 pc. The original distributions are presented in the two upper panels of Fig. 4, the maps smoothed with a 360 pc-beam are shown in the two bottom panels of Fig. 4. As expected, no relation between $\Sigma^{\rm UV}_{\rm SFR}$ and $\Sigma_{\rm gas}$ can be found for original simulated maps with high spatial resolution (the top right panel in Fig. 4). At the same time, a remarkable relation appears for smoothed data (the bottom right panel in Fig. 4). The locus of points for the simulated data is close to that for the extragalactic observations by Bigiel et al. (2010). Note that the spatial resolution in these observations is about 200–400 pc. Hence, to obtain the $\Sigma^{\rm UV}_{\rm SFR} - \Sigma_{\rm gas}$ relation, the smoothing scale should be comparable with the size of individual star-forming complexes. A comparison of the relations shown

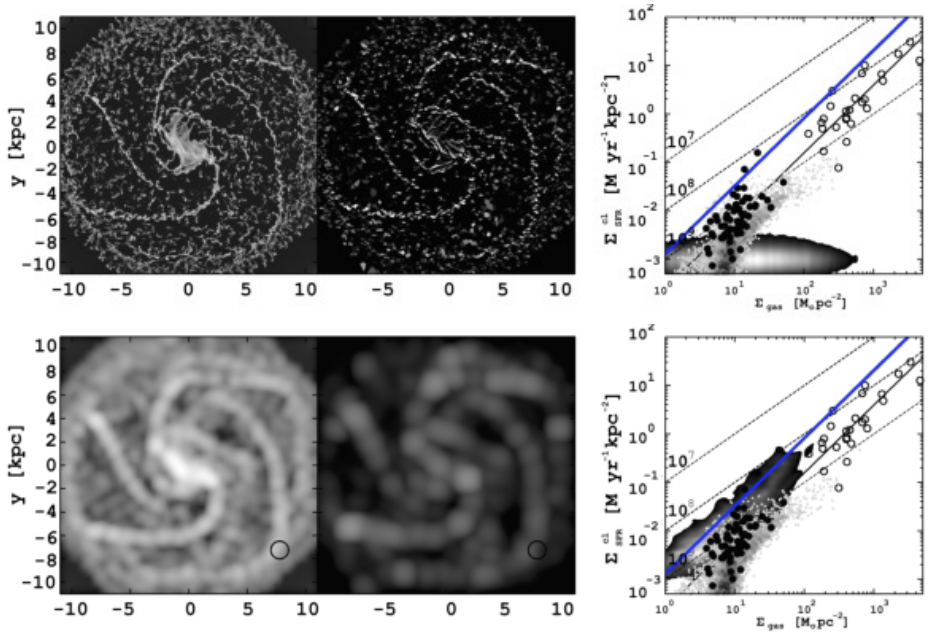

Fig. 4. The two maps on the left represent the gas surface density $\Sigma_{\rm gas}$ (the left-hand map) and the SFR surface density determined from UV flux, $\Sigma_{\rm SFR}^{\rm UV}$ (the right-hand map). The panels on the right show the $\Sigma_{\rm SFR}^{\rm UV} - \Sigma_{\rm gas}$ relation (black-white color map). Other designations are the same as in Fig. 3. The upper row of panels corresponds to the original simulated data, the bottom row represents the maps and the relation after the smoothing procedure with a Gaussian beam size of 360 pc (this size is shown by the black circle in the right bottom corner of the maps).

in Figs. 3 and 4 leads one to conclude that the relation based on free-fall time and that obtained using UV calibration for smoothed data have similar slopes, but for the latter the locus of points shifts to lower values of both gas surface density and surface SFR.

5. CONCLUSIONS

We used N-body/hydrodynamic simulations to study a sample of giant molecular clouds and star formation rate in a Milky Way-type galaxy. In this paper we show that

1. The dark gas fraction averaged over the whole sample of molecular clouds reaches about 30% by mass.

2. The conversion factors, $X_{\rm CO}$, for individual clouds deviate a factor of several times from the mean value for the MW clouds, 2×10^{20} cm^{-2} (K km s^{-1})$^{-1}$.

3. The $\Sigma_{\rm SFR}^{\rm UV} - \Sigma_{\rm gas}$ relation can be reproduced using UV calibration for smoothing scale compared to the size of individual star-forming complexes, $\sim 0.3 - 1$ kpc.

ACKNOWLEDGMENTS. Numerical simulations were performed at the Research Computing Center (Moscow State University) and supported by the Russian Science Foundation project (14-22-00041, "VOLGA – A View On the Life of GAlaxies"). This work was also partially supported by the Russian Foundation for Basic Research (grants Nos. 14-02-00604, 15-02-06204, and 15-32-21062). The thermo-chemical part was developed with the support by the Russian Scientific Foundation (14-50-00043). SAK acknowledges the support from the President of the RF program (MK-4536.2015.2). EOV is grateful to the Ministry of Education and Science of the Russian Federation (project 213.01-11/2014-5) and the Russian Foundation for Basic Research (project 15-02-08293).

REFERENCES

Bigiel F., Leroy A., Walter F. et al. 2010, AJ, 140, 1194
Bolatto A. D., Wolfire M., Leroy A. K. 2013, ARA&A, 51, 207
Colombo D., Hughes A., Schinnerer E. et al. 2014, ApJ, 784, 3
Duarte-Cabral A., Dobbs C. L. 2016, MNRAS, 458, 3667
Efremov Y. N. 1995, AJ, 110, 2757
Feldmann R., Gnedin N. Y., Kravtsov A. V. 2012, ApJ, 758, 127
Kennicutt R. C. 1998, ApJ, 498, 541
Kennicutt R. C., Evans N. J. 2012, ARA&A, 50, 531
Khoperskov S. A., Vasiliev E. O., Sobolev A. M., Khoperskov A. V. 2013, MNRAS, 428, 2311
Khoperskov S. A., Vasiliev E. O., Khoperskov A. V., Lubimov V. N. 2014, Journal of Physics Conference Series, 510(1), 012011
Khoperskov S. A., Vasiliev E. O., Ladeyschikov D. A. et al. 2016, MNRAS, 455, 1782
Leitherer C., Schaerer D., Goldader J. D. et al. 1999, ApJS, 123, 3
Nelson R. P., Langer W. D. 1999, ApJ, 524, 923
Pan H.-A., Fujimoto Y., Tasker E. J. et al. 2016, MNRAS, 458, 2443
Schmidt M. 1959, ApJ, 129, 243
Shchekinov Yu. A. 2004, Astrophysics, 47, 205
Smith R. J., Glover S. C. O., Clark P. C. et al. 2014, MNRAS, 441, 1628
Williams J. P., de Geus E. J., Blitz L. 1994, ApJ, 428, 693
Wolfire M. G., Hollenbach D., McKee C. F. 2010, ApJ, 716, 1191